Electron-phonon coupling on strained Ge/Si(111)-(5×5) surfaces

M. Stoffel,[1,2,*] Y. Fagot-Révurat,[1] A. Tejeda,[1,2] B. Kierren,[1] A. Nicolaou,[2] P. Le Fèvre,[2] F. Bertran,[2] A. Taleb-Ibrahimi,[2] and D. Malterre[1]

[1]*Université de Lorraine, UMR CNRS 7198, Institut Jean Lamour, BP 239, F-54506 Vandoeuvre-lès-Nancy, France*

[2]*Synchrotron SOLEIL, Cassiopée beamline, BP 48, 91192 Gif-sur-Yvette, France*

(Received 4 July 2012; revised manuscript received 31 October 2012; published 30 November 2012)

We investigate the structural and electronic properties of strained Ge/Si(111)-(5 × 5) surfaces by means of scanning tunneling microscopy and high-resolution angle-resolved photoemission spectroscopy. The homogeneous (5 × 5) reconstructed overlayers are characterized by three electronic surface states, similar to the Si(111)-(7 × 7) surface. The dispersion of the dangling bond related surface state exhibits the same periodicity as that of the (5 × 5) reconstruction. Moreover, a careful analysis of the shape and width of this surface state provides striking evidence of electron-phonon coupling at low temperatures. By considering the spectral function within a simple Debye model, we determine both the Debye energy and the electron-phonon coupling strength. The latter value is further confirmed by analyzing the temperature-dependent phonon broadening of the dangling bond related surface state linewidth.

DOI: 10.1103/PhysRevB.86.195438 PACS number(s): 79.60.Bm, 68.37.Ef

I. INTRODUCTION

Electron-phonon coupling is a fundamental property in solid state physics since it determines among others the pairing of electrons in conventional superconductors. For this reason, extensive studies have been first conducted on bulk metals.[1] Later on, high-resolution angle-resolved photoemission spectroscopy (ARPES) has emerged as a powerful technique to probe the electron-phonon interaction also at surfaces and interfaces.[2,3] A typical example is given by photoemission studies on Be(0001) surfaces, which gave evidence of a rather strong coupling between the Γ surface state and the surface phonon modes.[4,5] The coupling strength was found to be larger compared to bulk samples, thus raising new questions concerning many-body physics in low-dimensional systems. The electron-phonon interaction was then studied experimentally on surfaces of metals[6–9] and semimetals.[10,11] In parallel to experimental studies, theoretical works based on a calculation of the Eliashberg spectral function gave access to the coupling strength on various metal surfaces.[12,13] First-principle calculations were also performed to determine the strength of the electron-phonon coupling on either free-standing monolayers,[14,15] bilayer graphene,[16] or very recently in alkali metals such as bcc lithium.[17] Surprisingly, there are only a few reports on electron-phonon interaction on semiconductor surfaces. This is mainly due to the fact that, unlike metals, there are no bands crossing the Fermi level. Barke *et al.*[18] used ARPES to give evidence of electron-phonon coupling on Si(111)-(7 × 7) surfaces. The different determinations yield a coupling strength of about 1.0–1.1, which indicates a rather strong coupling. This result, together with a bandwidth reduction, makes this surface an ideal playground for investigating many-body effects. The obtained results naturally raise the question whether electron-phonon interaction could also be important on other semiconductor surfaces or interfaces. Besides Si, Ge-based materials have gained a tremendous interest in the last years due to potential applications in future micro/nanoelectronic devices[19] or in photonics.[20] A detailed understanding of the electronic properties of Ge/Si interfaces is therefore of paramount importance. When about 2–3 monolayers of Ge are deposited on Si(111) surfaces at substrate temperatures between 450 and 550 °C, the surface reconstruction is known to change from (7 × 7) to (5 × 5). The structural properties of (5 × 5) reconstructed overlayers have been characterized by scanning tunneling microscopy (STM).[21,22] Moreover, the electronic properties of these surfaces have been already studied by ARPES[23] revealing three electronic surface states, similar to what has been reported for Si(111)-(7 × 7) surfaces.

From a fundamental point of view, it would be interesting to know how the electron-phonon coupling strength is modified at an interface of two elemental semiconductors like Ge/Si. Ge has a larger lattice constant than Si as a result, a Ge thin film will be strained (4.2% misfit) on the Si(111) substrate. The biaxial compressive strain may affect the structural/electronic properties of the surface and therefore also the strength of the electron-phonon interaction.

In this paper, we investigate the electron-phonon coupling on strained Ge/Si(111) wetting layers. The initial (7 × 7) reconstruction of the clean Si(111) surface exhibits a (5 × 5) reconstruction as soon as more than 1.5 monolayer (ML) Ge are deposited (at least for substrate temperatures higher than 450 °C). Larger coverages around 3 ML Ge leads to homogeneous (5 × 5) reconstructed overlayers. ARPES measurements reveal the presence of three surface states, similar to bare Si(111)-(7 × 7) surfaces. The dispersion of the surface state closest to the Fermi level exhibits the same periodicity as the (5 × 5) reconstruction. Moreover, by considering the detailed shape and width of this state, we provide striking evidence of electron-phonon coupling at low temperatures. A fully analytical calculation of the spectral function within a simple Debye model allows us to determine both the electron-phonon coupling strength as well as the Debye energy. Finally, the temperature-dependent phonon broadening of the surface state linewidth yields a second determination of the coupling strength, which appears to be fully consistent with the first one. The paper is divided as follows: In Sec. II the experimental details will be presented. In Sec. III the structural properties will be presented and in Sec. IV the electronic properties

of Ge/Si(111) wetting layers will be discussed. Finally, the electron-phonon interaction is discussed in Sec. V before all results are summarized in Sec. VI.

II. EXPERIMENTAL DETAILS

The experiments were performed in an ultrahigh vacuum chamber which couples a preparation chamber equipped with low-energy electron diffraction (LEED) and Auger electron spectroscopy, a high-resolution ARPES chamber, and a low-temperature STM chamber. For our experiments we used *n*-type Si(111) substrates with a resistivity varying between 0.18 and 0.23 Ω cm. After *ex-situ* chemical cleaning in acetone/propanol, the samples were transferred into vacuum and outgassed for several hours at 700 °C. Once a base pressure of about 1×10^{-10} mbar is recovered, the Si(111) substrates were repeatedly flashed at 1200 °C prior to cooling down at 800 °C for 1 min followed by slow cooling to room temperature. This procedure allows us to obtain sharp (7 × 7) LEED patterns, which are indicative of oxide-free Si(111) surfaces. Nominally pure Ge was then subsequently deposited on top of Si(111) substrates using a Knudsen cell. The substrate was heated at 500 °C and the Ge rate was about 0.3 ML/min. The rate was calibrated by considering the onset of (5 × 5) spots in the LEED pattern. After deposition, the substrate temperature was immediately ramped down to room temperature. The surface morphology was then checked by LEED and by a STM operating at 77 K. ARPES measurements were performed with a Scienta SES 200 analyzer. The photon source is a Specs helium discharge lamp, which is monochromatized on the He I ($h\nu = 21.2$ eV) energy. For the measurements we used a pass energy of 10 eV and 0.5 mm slit width allowing a high signal to noise ratio. Under these conditions, the energy and angle resolution are 10 meV and 0.2°, respectively. The Fermi energy was measured on the molybdenum part of the sample holder. Temperature-dependent photoemission measurements and Fermi surface mapping were performed on the Cassiopée beamline at synchrotron SOLEIL.[24] The beamline is equipped with a modified Petersen PGM monochromator with a resolution $E/\Delta E \sim 70\,000$ at 100 eV and 25 000 for lower energies providing photon with energies between 8 and 1500 eV. For our measurements we used the high-resolution photoemission branch, which is equipped with a manipulator operating between 400 and 5 K and with a Scienta R4000 electron analyzer having a ±15° acceptance angle with a base energy resolution lower than 1 meV and 0.1° angular resolution. The resolution of both beamline and analyzer is estimated to be lower than 40 meV. The photoemission chamber is connected to a preparation chamber with surface science preparation and characterization techniques.

III. STRUCTURAL PROPERTIES OF Ge/Si(111)-(5 × 5) SURFACES

Figure 1(a) shows a typical LEED pattern obtained upon deposition of about 3 ML Ge on Si(111)-(7 × 7) at 500 °C. Apart from the spots corresponding to the ideal (1 × 1) surface (circled in white), we can identify several other spots indicating a (5 × 5) reconstruction (circled in red). As the Ge coverage increases, (5 × 5) related spots start to coexist with

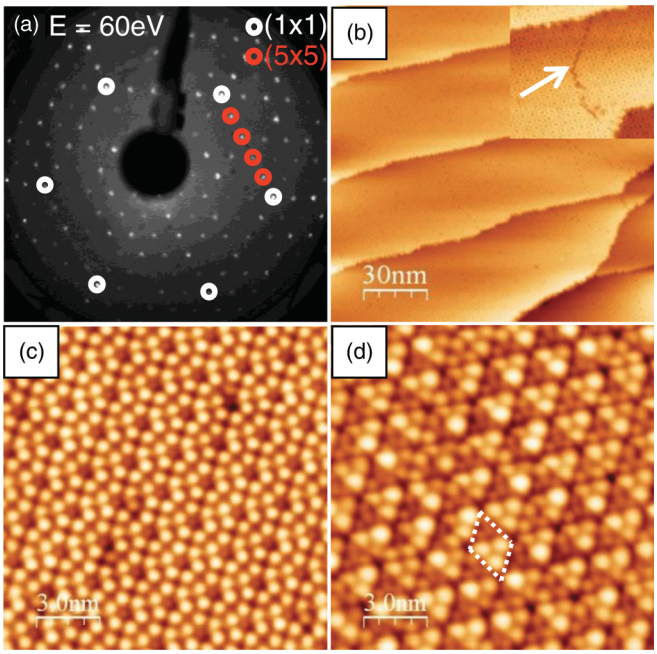

FIG. 1. (Color online) (a) LEED pattern taken at $E = 60$ eV after deposition of 3 ML Ge on Si(111)-(7 × 7) at 500 °C. (b) Large area (150 nm × 150 nm) STM scan taken at 77 K. A high-resolution STM image of a defect line (pointed at by a white arrow) is shown as an inset. High-resolution STM images (15 nm × 15 nm) taken at 77 K and probing (c) the unoccupied states (+1.37 V, 1 nA) and (d) the occupied states (−1.37 V, 1 nA). The unit cell of the (5 × 5) reconstruction is indicated by a white dashed line in (d).

(7 × 7) related spots, suggesting the coexistence of (5 × 5) and (7 × 7) reconstructed domains.[25–27] When the Ge deposition is stopped at about 3 ML, no traces of (7 × 7) domains can be detected, suggesting that a major part of the surface is (5 × 5) reconstructed. This is directly corroborated by STM investigations [Fig. 1(b)]. The large area scan shows the occurrence of terraces separated by steps. On the terraces, (5 × 5) reconstructed domains separated by defect lines can be identified [see inset of Fig. 1(b)]. These domains have recently gained a tremendous interest since they may act as templates for the growth of either In or Ga clusters.[28] The defect lines separating two adjacent domains have also been the subject of a detailed structural characterization.[29] They might originate from a partial strain relaxation, similar to the dimer vacancy lines observed when Ge is deposited on top of Si(001) substrates.[30] No traces of 3D island formation were detected in large area STM images taken at different surface locations. A better insight into the structural properties can be further gained from high-resolution STM images shown in Fig. 1(c) (unoccupied states) and Fig. 1(d) (occupied states). In the unoccupied state image, hexagon-like features are observed, similar to previous characterizations.[21,22] In the occupied state image, the unit cell is indicated by a white dashed line. The latter is divided into faulted and unfaulted half-unit cells. Each (5 × 5) half-unit cell contains three adatoms and a single restatom.[31] We further note that some adatoms appear brighter than their neighbors. This may be ascribed to Si intermixing in the surface layer as already suggested by Becker *et al.*[21] and Fukuda.[22] The structure of the (5 × 5) unit cell appears to be

consistent with a dimer-adatom-stacking fault model.[32] All the results discussed above thus suggest a structural analogy with the clean Si(111)-(7 × 7) surface in agreement with previous results from the literature.[33] In the following we will now consider the electronic properties of homogeneous, (5 × 5) reconstructed surfaces.

IV. ELECTRONIC PROPERTIES OF Ge/Si(111)-(5 × 5) SURFACES

Figure 2(a) shows the band structure of the Ge/Si(111)-(5 × 5) surface measured at room temperature along the $\bar{\Gamma}$-$\bar{K}$ line of the (1 × 1) surface Brillouin zone. The corresponding energy distribution curves are shown in Fig. 2(b). For binding energies down to ∼1.5 eV, one can distinguish three electronic states noted as S_1, S_2, and S_3. The first two states do not strongly disperse while the third one disperses downwards with a bandwidth of about 0.4 eV. For binding energies larger than ∼2 eV, the band structure is almost entirely dominated by a structure noted as B, which is due to emission from bulk states.[23] The dispersions of the three states S_1, S_2, and S_3 closest to the Fermi level are reported as open symbols in Fig. 2(c). The results are then compared with previous measurements by Mårtensson *et al.*[23] shown as full symbols. Although the Ge/Si(111)-(5 × 5) surfaces were prepared in a different way, a good agreement is found between the two independent measurements. We note that a more complete dispersion could be obtained in our case due to the improved resolution of our experimental setup. Based on the results of Mårtensson *et al.*,[23] we can thus attribute the states S_1, S_2, and S_3 to surface states associated with dangling bonds on adatoms, dangling bonds on restatoms, and adatom backbonds. A photon energy dependence further corroborates the surface character of the states S_1, S_2, and S_3 (not shown here). The structural analogy with the Si(111)-(7 × 7) surface discussed above thus translates into an analogy of the electronic properties. Both experimental studies[23,34,35] and recent *ab initio* calculations[36] indicate that the (5 × 5) surface is metallic, which offers the opportunity to probe the electron-phonon interaction.

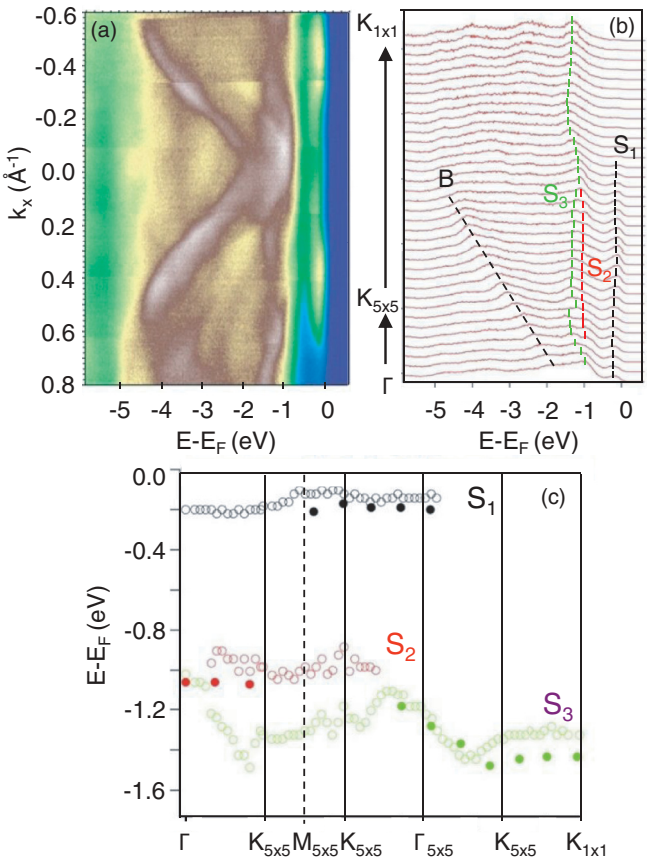

FIG. 2. (Color online) Ge/Si(111)-(5 × 5) band structure measured along the $\bar{\Gamma}$-$\bar{K}$ direction at (a) room temperature ($h\nu = 21.2$ eV) and (b) the corresponding energy distribution curves. The dispersion of three electronic states localized close to the Fermi level is indicated by black, red, and green lines. (c) Experimental dispersion of the states S_1, S_2, and S_3 (open symbols). The results are compared with former results by Mårtensson *et al.*[23] (full symbols).

In the following we measure for each surface state the corresponding equienergetic cut, that is, the band structure in the (k_x,k_y) plane at the energy corresponding to the surface state (relative to the Fermi level). Figure 3(a) shows the constant energy cut measured at room temperature at 110 meV from the Fermi level, which corresponds to the surface state S_1. The photon energy was set to 34 eV, which maximizes the cross section of the surface state. The surface Brillouin zones of the (5 × 5) reconstruction are superimposed on the band structure. In the case of a pure surface state, one would expect that the constant energy map exhibit a sixfold symmetry resulting from both the surface structure and from time-reversal symmetry. We observe three intense and three weak structures so that the spectral weight rather displays a threefold symmetry. Such an asymmetry in the spectral weight has already been observed for example in Ag/Si(111) and has been interpreted to result from selection rules and matrix elements.[37]

The intensity along the dashed line in Fig. 3(a) follows a series of alternating intensity maxima and minima while almost no intensity is found in other Brillouin zones. In order to tentatively explain the observed intensity distribution, we used a simple model based on the calculation of the structure factor.[38] The spectral weight distribution reflects the structure factor of the surface but not the periodicity of the (5 × 5) reconstruction. The result of the calculation is shown in Fig. 3(b). A detailed comparison with our experimental data shows that we are indeed able to reproduce qualitatively the alternating intensity maxima and minima along the dashed line. However, the latter are centered within the Brillouin zones [Fig. 3(b)], while experimentally they appear rather located at the edges between two neighboring Brillouin zones [Fig. 3(a)]. The differences may be explained by the fact that our model is probably oversimplified since possible distortions, height differences between unfaulted and faulted half unit cells, etc. are not taken into account.

As a next step, we analyze the photoemission intensity measured at $T = 6$ K along $k_y = 0$ in Fig. 3(a). The result is depicted in Fig. 3(c). The dispersion of the surface state S_1, which is shown as a red dashed line, is indeed periodic. This is better seen by considering a momentum distribution curve taken at the Fermi level [Fig. 3(d), upper curve]. The periodicity is about 0.4 Å^{-1}, which nicely fits with the expected periodicity deduced from the atomic structure of the (5 × 5) reconstructed surface ($2k_F^{5\times5} = 0.4$ Å^{-1}). Within a tight

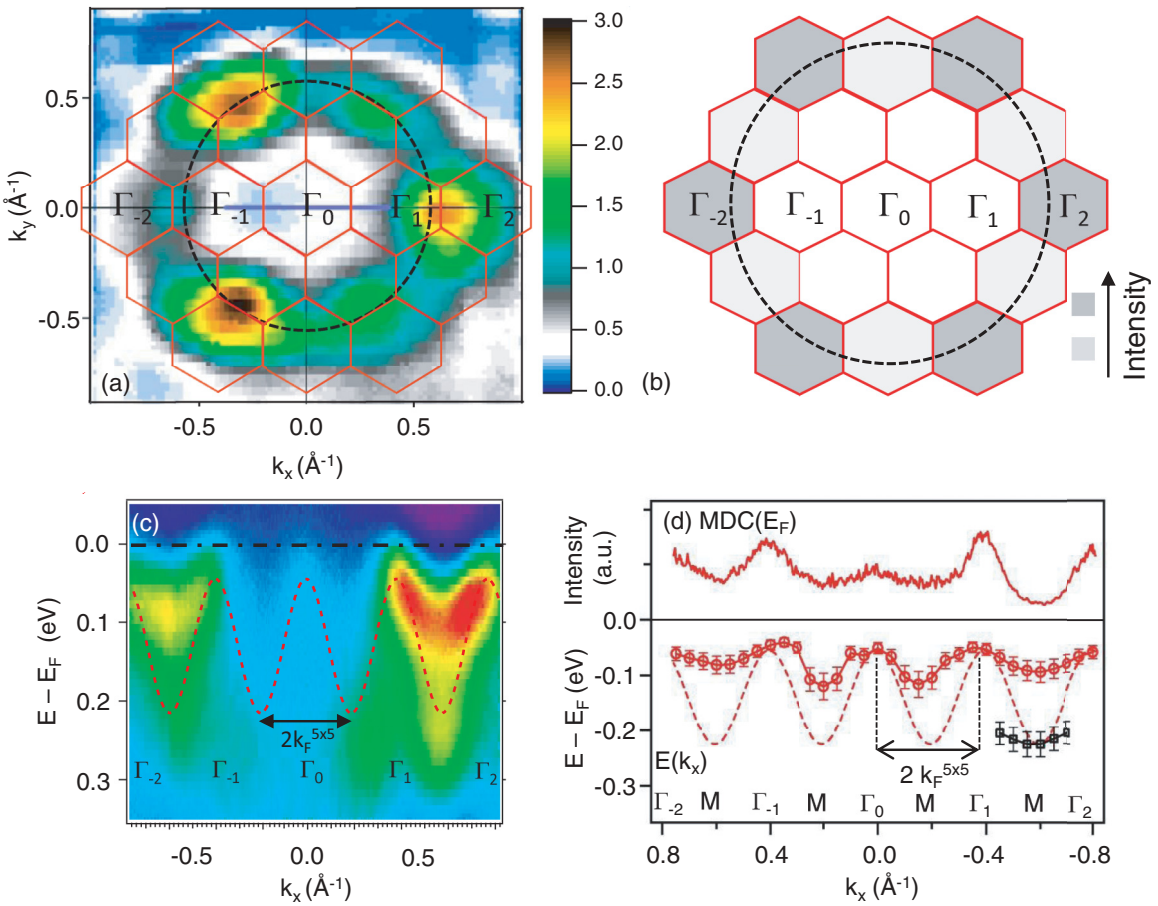

FIG. 3. (Color online) (a) Room temperature constant energy cut at $E - E_F = -110$ meV with $h\nu = 34$ eV. The (5×5) surface Brillouin zones (red hexagons) are superimposed. (b) Calculated intensity based on the structure factor (see text for details). (c) Photoemission intensity $I(k_x,k_y = 0)$ measured at $T = 6$ K. The Fermi level is indicated by a black dashed-dotted line while the dispersion of the surface state S_1 is indicated by a red dashed line. (d) Momentum distribution curve taken at $E = E_F$ in (c) (upper curve), experimental energy dispersion of the surface state S_1 (open symbols) (lower curve). The data are fitted by a cosine function (red dashed line, see text for details). The red solid line is a guide for the eye. The red and black dots are experimental points which correspond to the position of the "dressed" and "bare" peak shown in Fig. 4(b).

binding approach, the surface state dispersion can be modeled by a cosine function given by the following expression:

$$\varepsilon(k_x) = 0.1 \cos\left(\frac{\pi}{k_F^{5\times5}} k_x\right) - 0.1. \quad (1)$$

By using these parameters, we were able to reproduce correctly the dispersion of the surface state S_1 as shown in the lower part of Fig. 3(d). We note that while the dispersion is periodic, the spectral weight does not exhibit the same periodicity. Finally, it is interesting to note that the surface state does not cross the Fermi level but instead, it seems that a small, about (55 ± 5) meV large bandgap opens up. This value is directly obtained from the adjustment of the fit to the data in Fig. 4(b). In the following we will now focus our attention to the Γ_1-M-Γ_2 region in which the spectral weight reaches a maximum.

V. EVIDENCE OF ELECTRON-PHONON COUPLING

An enlargement of the Γ_1-M-Γ_2 region is shown in Fig. 4(a). Apart from the dispersion of the unperturbed surface state S_1 shown as a black dashed line, we note the presence of two intensity maxima in the spectrum indicated by red dashed lines. The slope of these lines is different from that of the unperturbed surface state dispersion (black dashed line). This result thus indicates a renormalization of the velocity close to the Fermi level. Cross sectional line scans taken at two different wave vectors are shown in Fig. 4(b). The experimental data, which are shown as open red symbols, can be nicely fitted with two Gaussian functions. When moving from $k_x = -0.59$ Å^{-1} to $k_x = -0.79$ Å^{-1}, we clearly observe a transfer of spectral weight from the "bare" to the "dressed" component.[4,18] This observation together with the velocity renormalization close to the Fermi level are clear experimental signatures of electron-phonon coupling on Ge/Si(111)-(5×5) surfaces. In the next step we will try to determine both the coupling strength and the Debye energy. In order to simulate the experimental photoemission data, we start with the spectral function. The latter is given by the following expression:[39]

$$A(\omega,k) = \frac{\pi^{-1} \left|\sum_I (\omega,k)\right|}{[\hbar\omega - \varepsilon(k) - \sum_R (\omega,k)]^2 + \sum_I (\omega,k)^2}, \quad (2)$$

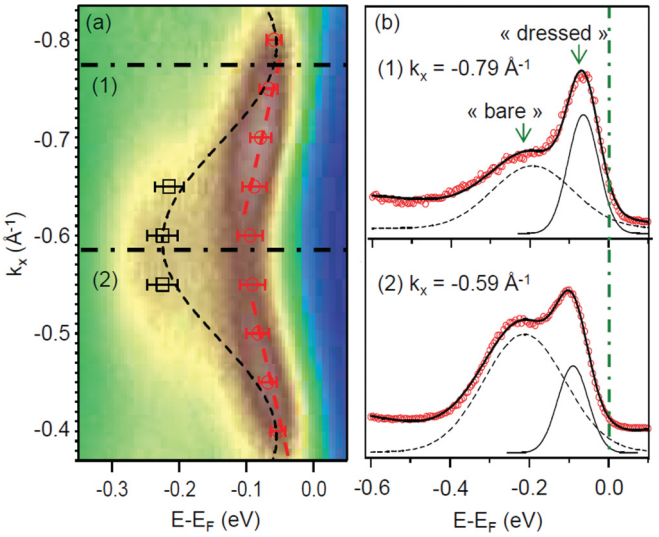

FIG. 4. (Color online) (a) Band structure measured at $T = 6$ K in the vicinity of the Fermi level with $h\nu = 34$ eV. The black dashed line represents the unperturbed surface state dispersion. The red dashed lines correspond to the dispersion of the surface state perturbed by the electron-phonon coupling, demonstrating the renormalization of the velocity near the Fermi level. (b) Line scans through the positions marked as (1) and (2) in (a). The experimental data (open red symbols) are fitted with two Gaussian curves. The result of the fit is shown as a solid line.

where $\varepsilon(k)$ is the unperturbed dispersion and Σ_R, Σ_I are the real and imaginary parts of the self-energy, respectively. Assuming that the latter depend only slowly on momentum, they are given by the following analytical expressions[39] within a simple Debye model:

$$\left|\sum_I(\omega)\right| = \frac{\hbar\lambda_{\text{e-ph}}\pi|\omega|^3}{3\omega_D^2}, \quad |\omega| < \omega_D, \tag{3}$$

$$\left|\sum_I(\omega)\right| = \frac{\hbar\lambda_{\text{e-ph}}\pi\omega_D}{3}, \quad |\omega| > \omega_D, \tag{4}$$

$$\sum_R(\omega) = -\frac{\lambda_{\text{e-ph}}\hbar\omega_D}{3}\left[\left(\frac{\omega}{\omega_D}\right)^3 \ln\left(\frac{\omega_D^2-\omega^2}{\omega^2}\right) + \ln\left(\frac{\omega_D+\omega}{\omega_D-\omega}\right) + \frac{\omega}{\omega_D}\right], \tag{5}$$

where $\lambda_{\text{e-ph}}$ is the electron-phonon coupling strength and ω_D is the Debye frequency. Under reasonable assumptions and at $T = 0$ K, the photoemission intensity is proportional to the spectral function.[40] This allows us to directly simulate the experimental spectrum. In a first step, we calculate both the real part and the imaginary part of the self-energy for different electron-phonon coupling strength (λ_{e-ph}) and Debye frequencies (ω_D). Both parameters were systematically varied until we were able to reproduce correctly the renormalization of the Fermi velocity [i.e., the slope of the red dashed lines in Fig. 4(a)]. The latter is about 0.03×10^8 cm/s (or 0.2×10^8 cm/s when not renormalized by the electron-phonon coupling). A good agreement is found for $\lambda_{\text{e-ph}} = (0.53 \pm 0.10)$ and $\hbar\omega_D = (0.08 \pm 0.02)$ eV. The error bars correspond to the interval that gives the same agreement with

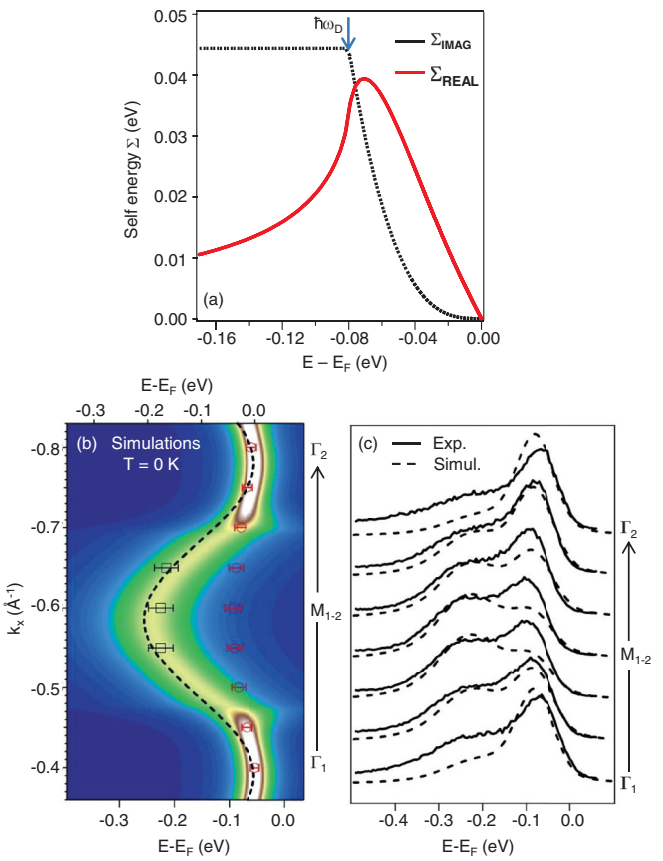

FIG. 5. (Color online) (a) Real part (red line) and imaginary part (black dotted line) of the self-energy calculated within Debye's model for the electron-phonon coupling strength and Debye energy which fit best our experimental data. (b) Simulated photoemission spectrum at $T = 0$ K (upper scale). The experimental data taken from Fig. 4 are superimposed. A qualitative agreement is found when the experimental data are shifted by about 70 meV (lower scale). The black dashed line corresponds to the unperturbed surface state dispersion along Γ_1-M-Γ_2. (c) Comparison between the experimental dispersion (solid lines) and the simulated dispersion (dashed lines) along Γ_1-M-Γ_2.

the experimental results. Both real and imaginary parts of the self-energy are plotted in Fig. 5(a). The electron-phonon coupling strength determines the slope of the real part of the self-energy near E_F, while the Debye energy [pointed at by an arrow in Fig. 5(a)] is deduced from the imaginary part of the self-energy. The electron-phonon coupling strength is within the range of most values reported in the literature (0.1–1.5).[2] The obtained value is nevertheless significantly smaller than the value obtained on the clean Si(111)-(7 × 7) surface ($\lambda_{\text{e-ph}} = 1.0 - 1.1$).[18] This result shows that the deposition of a very thin (i.e., 3 ML) Ge layer is already sufficient to strongly modify the electron-phonon interaction. In a second step, we then determine the spectral function which allows us to simulate the photoemission data. The simulated photoemission spectrum along Γ_1-M-Γ_2 is shown in Fig. 5(b). A good qualitative agreement is found with the experimental data when the latter are shifted by about 70 meV with respect of the simulated data. The physical origin of this shift is not yet clear. It comes from the fact that the low energy part of the surface

state dispersion never crosses the Fermi level due to the band folding caused by the (5×5) surface reconstruction. Such a shift has also been observed previously on Si(111)-(7×7) surfaces[18] and has not been really discussed in this paper. This could be due to a wrong position of the Fermi level due to a non-negligible band bending expected on metal/semiconducting interfaces. Finally, the experimental energy dispersion curves are compared with the simulated ones in Fig. 5(c). To correctly reproduce our experimental results, the simulated data were further convoluted with a Gaussian function having a width of about 0.2 Å^{-1} (i.e., much larger than the instrumental resolution which is lower than 0.02 Å^{-1}). Within these conditions, a qualitative agreement is found between the experimental and simulated dispersions. We note, however, that the experimental data cannot be perfectly fitted and that the spectral weight distribution is not correctly reproduced. This shows the limitation of our approach based on Debye's model. Alternatively, Einstein's model could also have been used. However, both models are known to qualitatively lead to similar results with comparable energy scales and electron-phonon coupling strength.[11] To get a better fit of our experimental results, more refined calculations should thus be performed taking into account both the k dependence of the electron-phonon coupling strength and the phonon density of states.

The electron-phonon coupling strength can be further determined from the phonon induced broadening of the photoemission peak linewidth with temperature. In the limit $k_B T \geqslant \hbar\omega_D$, the linewidth Γ is given by the following relation:[1]

$$\Gamma \approx 2\pi \lambda_{\text{e-ph}} k_B T. \tag{6}$$

In our case, however, the Debye energy is much larger than the thermal energy at room temperature (25 meV). Since many authors use the above equation even in the temperature range from 0 to 300 K,[7,18,41] we can also tentatively apply Eq. (6) for a second determination of the electron-phonon coupling strength. Figures 6(a)–6(c) displays the energy distribution curves taken at the same wave vector $k_x = -0.79$ Å^{-1} at three different temperatures. At low temperatures, surface photovoltage effects are known to occur. We therefore adjust the Fermi level at each temperature by considering the position of the core levels. The energy distribution curves (red lines) are well fitted with two Gaussian curves. For the fit, the center of the Gaussian is kept fixed while all other parameters are adjusted to optimize the fitting. It is obvious that the linewidth of the quasiparticle peak closest to the Fermi level increases with temperature. A similar behavior is observed for the other surface state peaks (not shown here). In Figs. 6(a)–6(c) the surface state S_1 does not cross the Fermi level. It is only the phonon induced linewidth broadening which contributes to the spectral weight at E_F, thus preserving the metallicity of the surface. More detailed investigations would be needed at this stage but they are beyond the scope of the present paper. Figure 6(d) displays the temperature dependence of the linewidth of the quasiparticle peak [indicated in blue in Figs. 6(a)–6(c)]. The obtained data can be nicely fitted with a straight line, yielding an electron-phonon coupling strength $\lambda_{\text{e-ph}} = (0.532 \pm 0.075)$. This result is in excellent agreement with the first determination using the simulation of the spectral function.

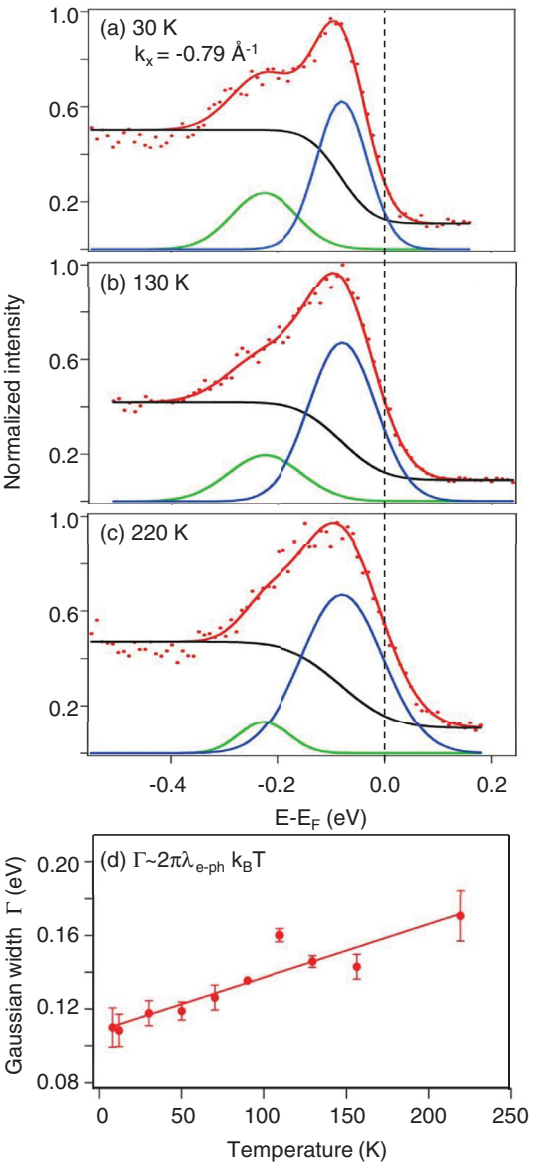

FIG. 6. (Color online) Normalized energy distribution curves (red lines) taken at $k_x = -0.79$ Å^{-1} for $T = 30$ K (a), 130 K (b), and 220 K (c). The experimental results are fitted with two Gaussian curves (indicated in green and blue). The base line is indicated in black. (d) Temperature dependence of the linewidth of the quasiparticle peak [indicated in blue in (a)–(c)].

VI. CONCLUSION

To summarize, we have analyzed both the structural and electronic properties of strained Ge/Si(111)-(5×5) surfaces. The dispersion of the dangling bond on adatom state was found to exhibit the same periodicity as that of the (5×5) reconstruction. Moreover, by considering the shape and the width of this surface state, we gave experimental evidence of electron-phonon coupling at low temperatures. A fully analytical calculation of the spectral function within a simple Debye model gave access to both coupling strength and Debye energy. The temperature dependence of the quasiparticle peak linewidth allowed a second determination of the coupling strength, which is fully consistent with the first one. We

expect that our results pave the way for engineering novel semiconductor interfaces with original electronic properties. Future work may consider the effect of strain on the electron-phonon coupling. This could be done either theoretically and/or experimentally by comparing our data with similar ARPES measurements on unstrained, bulk terminated Ge(111)-$c(2 \times 8)$ surfaces.

ACKNOWLEDGMENTS

The authors wish to thank Pavel Jelinek (Nanosurf Lab, Institute of Physics of the Academy of Sciences, Prague, Czech Republic) for fruitful discussions. This work was supported by the French Agence Nationale de la Recherche (ANR), project SurMott, ref. NT-09-618999.

*Corresponding author: mathieu.stoffel@ijl.nancy-universite.fr

[1] G. Grimvall, in *The Electron-Phonon Interaction in Metals*, edited by E. Wohlfarth, Selected Topics in Solid State Physics (North-Holland, New York, 1981).

[2] E. W. Plummer, J. Shi, S. J. Tang, E. Rotenberg, and S. D. Kevan, Prog. Surf. Sci. **74**, 251 (2003).

[3] Ph. Hofmann, I. Yu Sklyadneva, E. D. L. Rienks, and E. V. Chulkov, New J. Phys. **11**, 125005 (2009).

[4] M. Hengsberger, D. Purdie, P. Segovia, M. Garnier, and Y. Baer, Phys. Rev. Lett. **83**, 592 (1999).

[5] M. Hengsberger, R. Frésard, D. Purdie, P. Segovia, and Y. Baer, Phys. Rev. B **60**, 10796 (1999).

[6] P. Straube, F. Pforte, T. Michalke, K. Berge, A. Gerlach, and A. Goldmann, Phys. Rev. B **61**, 14072 (2000).

[7] D. A. Luh, T. Miller, J. J. Paggel, and T. C. Chiang, Phys. Rev. Lett. **88**, 256802 (2002).

[8] J. Kroger, Rep. Prog. Phys. **69**, 899 (2006), and references therein.

[9] C. Tournier-Colletta, B. Kierren, Y. Fagot-Révurat, and D. Malterre, Phys. Rev. Lett. **104**, 016802 (2010).

[10] H. Höchst and C. R. Ast, J. Electron Spectrosc. Relat. Phenom. **137-140**, 441 (2004).

[11] C. Kirkegaard, T. K. Kim, and Ph. Hofmann, New J. Phys. **7**, 99 (2005).

[12] A. Eiguren, B. Hellsing, F. Reinert, G. Nicolay, E. V. Chulkov, V. M. Silkin, S. Hüfner, and P. M. Echenique, Phys. Rev. Lett. **88**, 066805 (2002).

[13] A. Eiguren, B. Hellsing, E. V. Chulkov, and P. M. Echenique, Phys. Rev. B **67**, 235423 (2003).

[14] A. Leonardo, I. Yu Sklyadneva, P. M. Echenique, and E. V. Chulkov, Surf. Sci. **600**, 3715 (2006).

[15] A. Leonardo, I. Yu Sklyadneva, P. M. Echenique, and E. V. Chulkov, Surf. Sci. **601**, 4018 (2007).

[16] K. M. Borysenko, J. T. Mullen, X. Li, Y. G. Semenov, J. M. Zavada, M. B. Nardelli, and K. W. Kim, Phys. Rev. B **83**, 161402 (2011).

[17] T. Bazhirov, J. Noffsinger, and M. L. Cohen, Phys. Rev. B **84**, 125122 (2011).

[18] I. Barke, F. Zheng, A. R. Konicek, R. C. Hatch, and F. J. Himpsel, Phys. Rev. Lett. **96**, 216801 (2006).

[19] V. Jovanovic, C. Biasotto, L. K. Nanver, J. Moers, D. Grützmacher, J. Gerharz, G. Mussler, J. van der Cingel, J. J. Zhang, G. Bauer, O. G. Schmidt, and L. Miglio, IEEE Electron Device Lett. **31**, 1083 (2010).

[20] Y. Ishikawa and K. Wada, Thin Solid Films **518**, S83 (2010).

[21] R. S. Becker, J. A. Golovchenko, and B. S. Swartzentruber, Phys. Rev. B **32**, 8455 (1985).

[22] T. Fukuda, Surf. Sci. **351**, 103 (1996).

[23] P. Mårtensson, W. X. Ni, G. V. Hansson, J. M. Nicholls, and B. Reihl, Phys. Rev. B **36**, 5974 (1987).

[24] See beamline website: http://www.synchrotron-soleil.fr/Recherche/LignesLumiere/CASSIOPEE, for information.

[25] K. Kajiyama, Y. Tanishiro, and K. Takayanagi, Surf. Sci. **222**, 38 (1989).

[26] N. Motta, A. Sgarlata, R. Calarco, Q. Nguyen, J. Castro Cal, F. Patella, A. Balzarotti, and M. De Crescenzi, Surf. Sci. **406**, 254 (1998).

[27] B. Voigtlaender, Surf. Sci. Rep. **43**, 127 (2001).

[28] J. M. Mac Leod, D. Psiachos, A. G. Mark, M. J. Stott, and A. B. McLean, J. Phys. Conf. Ser. **61**, 800 (2007).

[29] A. G. Mark and A. B. McLean, Phys. Status Solidi C **7**, 185 (2010)

[30] U. Köhler, O. Jusko, B. Müller, M. Horn-von-Hoegen, and M. Pook, Ultramicroscopy **42-44**, 832 (1992).

[31] G. X. Qian and D. J. Chadi, J. Vac. Sci. Technol. B **4**, 1079 (1986).

[32] K. Kajiyama, Y. Tanishiro, and K. Takayanagi, Surf. Sci. **222**, 47 (1989).

[33] E. G. McRae, H. J. Gossmann, and L. Feldman, Surf. Sci. **146**, L540 (1984).

[34] T. Miller, T. C. Hsieh, and T. C. Chiang, Phys. Rev. B **33**, 6983 (1986).

[35] J. A. Carlisle, T. Miller, and T. C. Chiang, Phys. Rev. B **49**, 13600 (1994).

[36] D. Psiachos and M. J. Stott, Phys. Status Solidi B **244**, 3143 (2007).

[37] V. Pérez-Dieste, J. F. Sánchez-Royo, J. Avila, M. Izquierdo, L. Roca, A. Tejeda, and M. C. Asensio, Surf. Sci. **601**, 742 (2007).

[38] W. Srour, A. Tejeda, A. Nicolaou, P. Le Fèvre, F. Bertran, A. Taleb-Ibrahimi, and D. Malterre, J. Electron. Spectrosc. Relat. Phenom. (in press), doi: 10.1016/j.elspec.2012.08.005.

[39] S. LaShell, E. Jensen, and T. Balasubramanian, Phys. Rev. B **61**, 2371 (2000).

[40] G. Borstel, Appl. Phys. A **38**, 193 (1985).

[41] B. A. McDougall, T. Balasubramanian, and E. Jensen, Phys. Rev. B **51**, 13891 (1995).